https://doi.org/10.1016/j.rser.2020.109877

Photo-assisted non-aqueous lithium-oxygen batteries: progress and prospects

Peng Tan[1,*], Xu Xiao[1], Yawen Dai[2], Chun Cheng[2], Meng Ni[2,*]

1 Department of Thermal Science and Energy Engineering, University of Science and Technology of China, Hefei 230026, Anhui, China.
2 Department of Building and Real Estate, The Hong Kong Polytechnic University, Hung Hom, Kowloon, Hong Kong, China.
*Corresponding author
E-mail addresses: pengtan@ustc.edu.cn (Peng Tan), meng.ni@polyu.edu.hk (Meng Ni)

Abstract: Developing effective energy storage systems is crucial for the successful implementation of solar energy. Recently, incorporating suitable photocatalysts into the electrodes to form photo-assisted non-aqueous lithium-oxygen batteries significantly decreases the overpotentials and improves energy efficiency, providing a striking way of utilizing solar light. Focusing on this design, this work provides a timely summary of the latest progress and the remaining challenges of photo-assisted non-aqueous lithium-oxygen batteries. The working mechanisms and battery configurations are first introduced. Then, the advances in the photocatalyst materials are detailedly summarized, and the influence of illumination on the electrolyte is also reviewed. Moreover, the optimization of the operating protocols for extending the cycle life is also discussed. Future research should focus on the photocatalyst explorations, battery structure design, and operating management. The insights obtained from these investigations also benefit the development of other energy storage systems for the wide application of solar energy.

Keywords: Photo-assisted; Lithium-oxygen battery; Solar energy; Photocatalyts; Electrode design.

1. Introduction

With the ever-increasing concerns on the energy and environmental issues, developing renewable and clean energy becomes an urgent demand. Solar energy has been regarded as the most promising one owing to the great amount that can satisfy the global energy consumption completely [1]. To this end, various energy conversion technologies that transform solar energy into other forms have been developed and quickly attracted the society's attention, such as photovoltatic cells that produce electric energy [2] and photothermic systems that produce thermal energy [3,4]. However, the intermittent nature of solar energy hinders the wide application. Thus, it is crucial to search for energy storage systems that can store solar energy efficiently for continuous use [5].

Among various energy conversion systems, using the electrochemical method to convert solar energy into chemical energy has become a hot research topic owing to the high scale-flexibility, efficiency, and cost-effectiveness [6]. Rechargeable batteries can effectively achieve the conversion between chemical and electric energy, which are regarded as a possible solution for solar energy storage [7]. Among them, flow batteries, such as vanadium redox flow batteries (VRFBs) and Fe-Cr flow batteries [8], have attracted extensive research for their high efficiency, excellent scalability, and long lifetime [9–11]. However, suffering from the limited solubility of active materials in the electrolyte, the low energy density of flow batteries (e.g., ~25 Wh L^{-1} for VRFBs) hinders the practical applications [12]. Although lithium-ion batteries own a remarkable energy density (~300 Wh kg^{-1}), the value is still far from the

storage demand [13]. In comparison, rechargeable metal-air batteries exhibit great potential [14]. In such batteries, metal is one reactant, while oxygen is obtained from ambient air instead of occupying the volume or mass of the battery, and thus the theoretical energy density can be greatly improved [15]. For lithium-oxygen (Li-O_2) batteries based on non-aqueous electrolytes, the theoretical capacity (3862 mAh g^{-1}) and the equilibrium potential (2.96 V) gives an ultrahigh energy density of 11400 Wh kg^{-1} [16–18].

Using rechargeable batteries for solar energy storage is conventionally based on the strategy of storing the electric energy generated from solar energy inside the battery, which is namely the combination of “solar to electric energy” and “electric to chemical energy”. Consequently, the batteries and solar cells are two independent components, and the simple connection will inevitably lower the overall efficiency [19]. To address this issue, a novel strategy has been proposed in rechargeable batteries, which applies photocatalysts in the battery to use solar light for performance improvement [20]. Through this incorporation, the solar, electric, and chemical energy can be linked together in a single device, simplifying the system configuration and achieving the high efficiency. Based on this idea, various photo-assisted battery systems have been reported recently, including Li-ion, Li-O_2, Li-S, and other batteries [21–24]. Considering the striking feature of an ultra-high energy density, photo-assisted Li-O_2 batteries have undoubtedly attracted research interests and been developed rapidly. This strategy not only helps to store photo-energy in the discharge/charge process but also addresses the high overpotentials of conventional

Li-O_2 batteries, leading to significantly improved energy efficiency. Therefore, a timely summary of the progress and the remaining challenges is highly necessary for future development. Although excellent reviews on the photo-assisted batteries have been published recently [19,25], to our best knowledge, no works specifically concentrated on the photo-assisted Li-O_2 batteries have been made yet.

Thus, this article aims to provide an up-to-date snapshot of the latest progress and challenges of photo-assisted non-aqueous Li-O_2 batteries. It starts with the working mechanisms of photo-assisted charging and the corresponding battery configurations. Then, the advancements in the battery components, especially the photocatalyst materials, are detailedly introduced. Moreover, the influences of operating protocols on the behaviors and performance of the batteries are discussed. Finally, the remaining challenges and further perspectives are highlighted.

2. Working mechanisms and battery configurations

The basic mechanisms of non-aqueous Li-O_2 batteries during charge and discharge are the formation and decomposition of the solid product Li_2O_2 on the oxygen electrode [17]:

$$2Li^+ + 2e^- + O_2 \underset{\text{Charge}}{\overset{\text{Discharge}}{\rightleftharpoons}} Li_2O_2 \ (E = 2.96\ V) \qquad \text{(I)}$$

However, due to the low electrical conductivity, the charge voltage is high, which leads to both low energy efficiency and poor cycling stability as the electrolyte and electrode materials may be decomposed at a high voltage [26]. Thus, tremendous research efforts are made to lower the charge voltage, such as developing effective electrocatalysts and soluble redox mediators [27–32]. Among them, using

photo-assisted charging is proposed to reduce the charge voltage significantly, as schematically shown in Fig. 1.

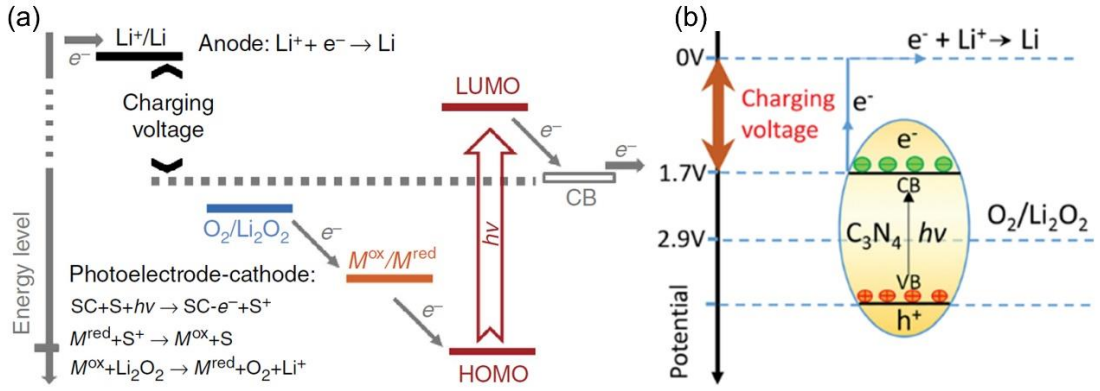

Fig. 1 Photo-assisted charging mechanisms in non-aqueous Li-O_2 batteries. (a) The energy diagram of a battery with a redox mediator. The SC and S represent semiconductor and sensitizer, respectively. Adapted with permission from Ref. [33]. (b) The theoretical potential diagram of a battery without a redox mediator. Adapted with permission from Ref. [34].

2.1 With redox mediator

Fig. 1a shows the energy diagram of a photo-assisted Li-O_2 battery during charge under illumination [33]. The dye molecules are excited by photons and then inject electrons into the conduction band (CB) of the photocatalyst. After that, the dye molecules become oxidized and are regenerated by receiving electrons from the reduced form of the redox mediator (M^{red}), which then becomes the oxidized form (M^{ox}) and transports to the oxygen electrode. The oxidized form of the redox mediator (M^{ox}) is reduced back to M^{red} by decomposing the solid Li_2O_2. Meanwhile, the electrons transport to the negative electrode to reduce Li^+ to form metallic Li. As a result, the battery returns to the initial state. Hence, the charge voltage can be

determined by the potential difference between the Li/Li^+ couple and the CB in the photoelectrode, which can be even lower than the equilibrium potential of Li-O_2 batteries (2.96 V).

2.2 Without redox mediator

Although the redox mediator contributes to reducing the charge voltage, it can transport to the Li electrode and be reduced [35], causing an internal shuttle phenomenon and decreasing the utilization of active mass [36]. In addition, the high concentration of redox mediators can also lead to undesired side reactions such as LiOH, affecting the reversibility [37,38]. To address these issues, the photo-assisted charging without the employment of redox mediators has been developed. The working mechanism of this approach is schematically illustrated in Fig. 1b, in which carbon nitride (C_3N_4) is taken as an example [34]. It is excited by photons to generate electrons and holes. The photoexcited holes can oxidize Li_2O_2 at the oxygen electrode due to the higher potential of the valence band (VB), and electrons reduce Li^+ to metallic Li at the Li electrode. Thus, based on this mechanism, the solid Li_2O_2 can be oxidized directly by the photocatalyst, improving efficiency and stability.

Based on the above two mechanisms, the battery configurations can be classified as two types. The first type is composed of a Li electrode, an oxygen electrode, and a photoelectrode, as schemed in Fig. 2a [33]. During discharge, oxygen reduces at the oxygen electrode. During charge, the photo-electrochemical oxidation starts on the photoelectrode first, producing the oxidized form of the redox mediator, which then transports to the oxygen electrode and further oxidizes the discharge product Li_2O_2.

Thus, the discharge and charge processes involve different working electrodes, and the redox mediator is the bridge to link the reactions on both electrodes. The other type is composed of a Li electrode and an oxygen electrode, and a separator may be applied to avoid the contact between the two electrodes, as schemed in Fig. 2b [39]. The catalyst materials on the oxygen electrode work for both oxygen electrocatalysis and photochemical reactions. Owing to the simple structure that is similar to that of conventional Li-O_2 batteries, this configuration has been widely applied in recently reported photo-assisted Li-O_2 batteries.

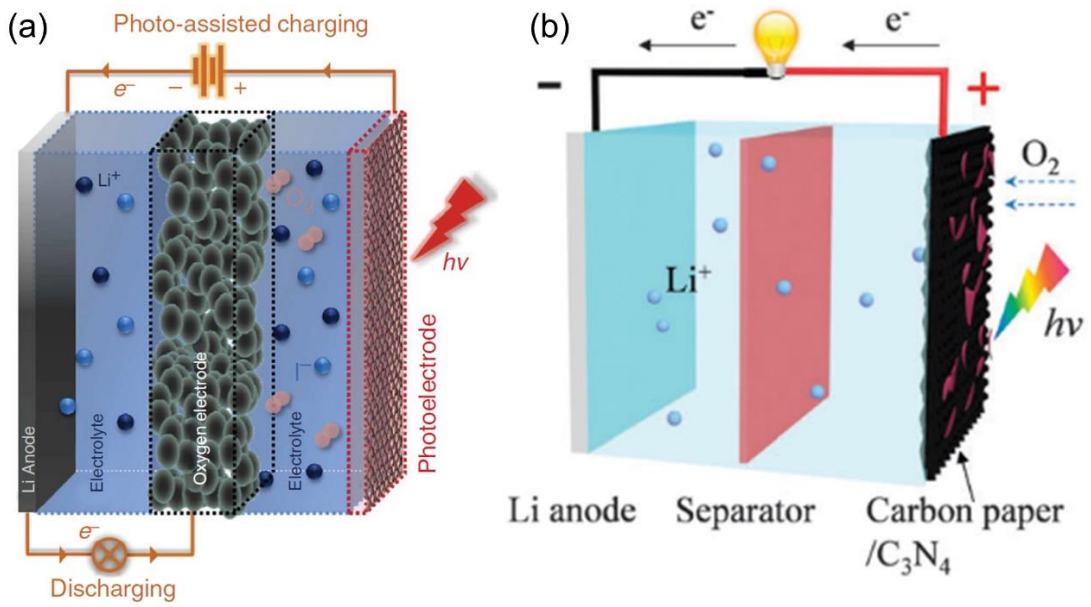

Fig. 2 Configuration of a photo-assisted rechargeable lithium-oxygen battery. (a) Three-electrode structure composed of a Li electrode, an oxygen electrode, and a photoelectrode. Adapted with permission from Ref. [33]. (b) Two-electrode composed of a Li electrode and an oxygen electrode with the photocatalyst. Adapted with permission from Ref. [39].

3. Battery materials for photo-assisted charging

In most reported solar-assisted rechargeable Li-O_2 batteries, lithium is directly

applied as the negative material to ensure the high capacity (3862 mAh g^{-1}). To solve the passivation and dendrite growth issues [40,41], Li_xSi has been applied and delivered a capacity close to the Li metal (3350 mAh g^{-1}) [42]. Besides the negative electrode materials, the photocatalyst materials are the key, and the electrolytes used in the batteries are also important to the electrochemical performance, which are detailedly introduced in this section.

3.1 Photocatalyst materials

For photo-assisted Li-O_2 batteries, the CB potential of the photoelectrode material should be as low as possible to reduce the charge voltage, while the VB potential should be more positive to oxidize Li_2O_2 to produce Li^+ and O_2. Besides, as the photocatalyst applied in the oxygen electrode, high activity toward oxygen electrocatalysis is also preferred. Based on these requirements, Table 1 summarizes the photocatalysts that have been used in photo-assisted Li-O_2 batteries.

Table 1 Summary of photocatalyst materials in photo-assisted Li-O_2 batteries and the corresponding electrochemical performance.

Photocatalyst material	Conduction band potential (V)	Electrolyte	Current density (mA cm^{-2})	Charge voltage (V)	Cycle number	Total time (h)	Ref.
Dye-sensitized TiO_2 nanorods on Ti gauze	~2.6	1 M $LiClO_4$/ DMSO with 0.1 M LiI	0.016 0.032	2.72 2.83	4	8	[33]
TiO_2 nanorod arrays	2.6	0.5 M $LiClO_4$/TEGDME	0.01 0.02 0.05	2.85 ~2.86 2.95	30	60	[43]
TiN/TiO_2 nanowires	~2.6	1 M $LiCF_3SO_3$/TEGDME	-	2.94 (midpoint)	120 (without light)	480	[44]
g-C_3N_4 on Ti	1.7	0.5 M	0.01	1.9	50	100	[39]

mesh		$LiClO_4$/TEGDME with 0.05 M LiI	0.02 0.03	~2.1 2.23			
g-C_3N_4 on carbon paper	1.7	1 M LiTFSI/TEGDME	0.01 0.03 0.05	1.96 ~2.1 2.4	70	140	[34]
C_3N_4 on carbon paper	1.7	0.5 M $LiClO_4$/TEGDME	0.04 0.08 0.10 0.15	~3.38	10	20	[45]
$CoSe_2$@g-C_3N_4	2.7	0.5 M $LiClO_4$/TEGDME	0.3	3.73	-	-	[46]
ZnS@CNT	~1.9	5 wt% LiTFSI/SCN	0.026 0.13 0.2	2.08 ~2.2 2.5	50	100	[42]
CdSe/ZnS QD@CNT	~2.0	1 M LiTFSI/TEGDME	0.1	4.07 (terminal)	over 100 (~40 under light)	200	[47]
WO_3 nanowire arrays	3.53	0.5 M $LiClO_4$/TEGDME	0.06	3.55	100	200	[48]

Motivated by the dye-sensitized TiO_2 solar cells, rutile TiO_2 nanorods sensitized by the Ruthenizer 535 bis-TBA dye molecules (N719) is applied as the photocatalyst. With the coupling of the I^-/I_3^- redox mediator, the charge voltage is significantly reduced to 2.72 V under illumination [33]. In addition, defective TiO_2 nanorod arrays grown on carbon textiles are also applied [43]. As the scan electron microscope (SEM) image shown in Fig. 3a, the textile surface is covered by many TiO_2 nanorods vertically grown on the textile to form aligned arrays. The high-resolution transmission electron microscope (HRTEM) image in Fig. 3b demonstrates that the TiO_2 nanorod has a diameter of ~200 nm and a length of ~1 μm. From Fig. 3b inset, the lattice spacing of 0.247 nm corresponds to the (101) plane, and some blurred areas can also be observed, indicating the presence of oxygen vacancies. When equipped in a Li-O_2 battery, the charge voltage reaches 4.31 V at the dark condition, and the

battery is cycled for only 14 times. With the light illumination, the charge and discharge voltages are about 2.86 V and 2.65 V for the first cycle, respectively, and change to 3.03 V and 2.85 V after 30 cycles, respectively. The remarkable performance may come from the generation of more defections and oxygen vacancies during the cycling process, improving the ORR performance and enhancing the migration of electrons and Li^+ ions. Furthermore, porous TiN/TiO_2 composite nanowires grown on carbon cloth are also applied in a $Li\text{-}O_2$ battery, which can maintain the voltage of above 2.0 V after 120 cycles without light [44]. When operated under illumination, the charge midpoint voltage decreases from 3.65 V to only 2.94 V, leading to the high energy efficiency of ~94%. Thus, the electron-hole pair generated on the excited electrode surface of TiN/TiO_2 helps to effectively oxidize Li_2O_2 during charge and compensates the electric energy.

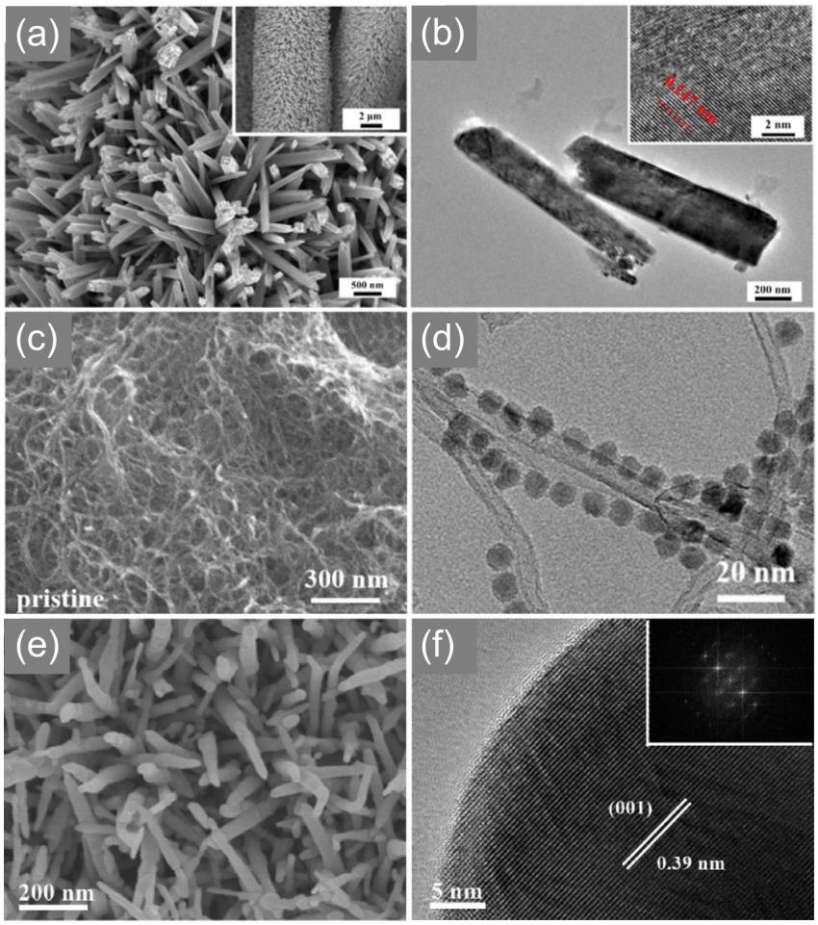

Fig. 3 Characterization of some photocatalyst materials applied in photo-assisted non-aqueous lithium-oxygen batteries. (a) SEM and (b) HRTEM images of the TiO_2/carbon textile composite, and the inset shows the lattice fringe of TiO_2. Adapted with permission from Ref. [43]. (c) SEM and (d) HRTEM image of CdSe/ZnS QDs@CNT composite. Adapted with permission from Ref. [47]. (e) SEM and (f) HRTEM images of WO_3, and the inset shows the Fourier filtered lattice fringe. Adapted with permission from Ref. [48].

Although TiO_2-based materials can effectively reduce the charge voltage under illumination, the CB potential is as high as 2.6 V, limiting the room for further improvement. In comparison, graphitic carbon nitride (g-C_3N_4), which features a CB potential of only 1.7 V, may become a promising photocatalyst material in

photo-assisted Li-O_2 batteries [39]. Owing to the high photocatalytic activity and remarkable oxygen electrocatalytic activity, when coupling with the I^-/I_3^- redox mediator, the charge voltage can be lowered to 1.9 V under illumination, leading to significant energy efficiency. Even without the employing of a redox mediator, g-C_3N_4 grown on carbon paper fibers with a coating structure can also achieve a charge voltage of 1.96 V and the energy efficiency of ~140% [34]. In addition to g-C_3N_4, a composite made of $CoSe_2$ and g-C_3N_4 is explored in which $CoSe_2$ nanorods with the length of 60~200 nm and an average width of ~50 nm are coated by a thin g-C_3N_4 sheet to form dendrite-like clusters [46]. Under a conventional charge process, the combination of $CoSe_2$ and g-C_3N_4 decreases the charge voltage by 280 mV, which may be caused by the synergistic effect of these two materials for oxygen electrocatalysis. While under the solar light, the charge voltage is further reduced by 170 mV due to the photoexcited holes that directly oxidize the discharge product. It is noticed that C_3N_4 is generally regarded as the photocatalyst for charging, while its functions in the discharge process have also been demonstrated recently [45]. When the battery is discharged under light, the photoelectrons generated in CB are capture by O_2 to form O_2^-, which then combines with Li^+, facilitating the formation of Li_2O_2. As shown in Fig. 4a, the discharge voltage is increased to 3.22 V, which is rather higher than the equilibrium potential of 2.96 V, suggesting that photo-energy is converted to electricity. Upon charging, the voltage is decreased to 3.38 V under light, indicating the effectiveness of C_3N_4 for the oxidation of Li_2O_2. Fig. 4b displays the voltage profiles under illumination at different current densities. Even the current

density increases from 0.04 to 0.15 mA cm^{-2}, the discharge and charge voltages are still around 3.22 and 3.38 V, respectively, with slight polarizations, demonstrating the efficient generation and facile transport of photoelectrons and holes in C_3N_4. Moreover, as shown in Fig. 4c, the discharge and charge overpotentials keep increasing without illumination, but stable voltage profiles are exhibited under illumination, illustrating the good stability for energy conversion and storage.

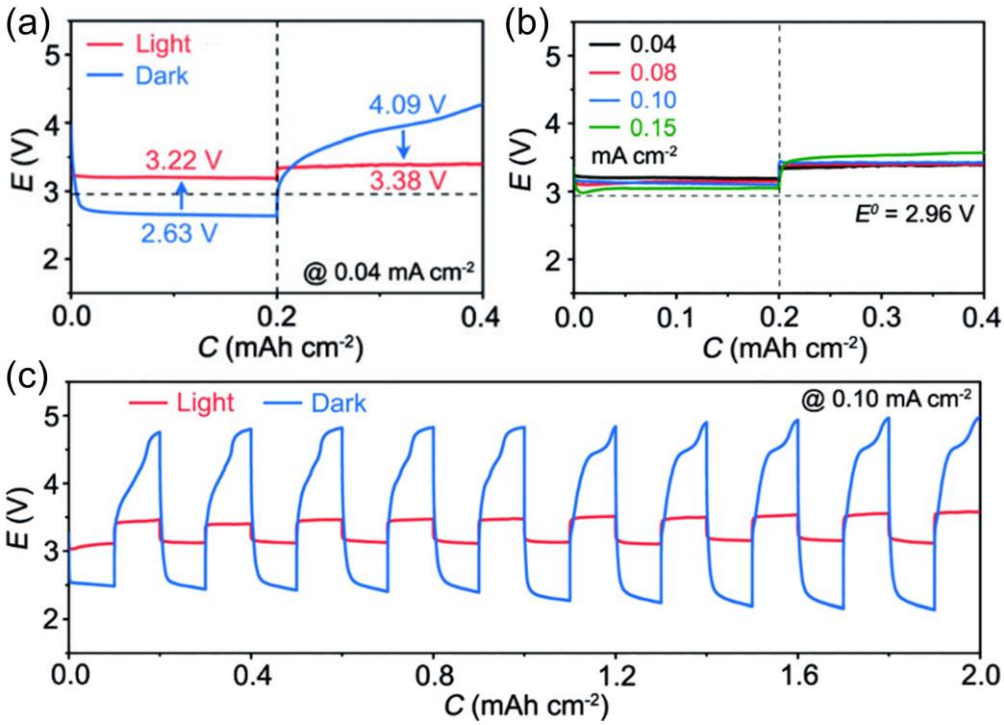

Fig. 4 Electrochemical performance of a Li-O_2 battery with C_3N_4 as the photocatalyst. (a) Discharge and charge voltage profiles with and without illumination at 0.04 mA cm^{-2}. (b) Voltage profiles under illumination at different current densities. (c) Cycling performance with and without illumination at 0.10 mA cm^{-2}. Adapted with permission from Ref. [45].

Besides, ZnS@CNT (carbon nanotube) composite is synthesized as the photocatalyst material, in which ~40 wt% ZnS spheres with the size of ~70 nm are

evenly distributed on the CNT surfaces. At a current density of 0.026 mA cm^{-2}, a typical high charge voltage of 4.09 V is exhibited, but greatly decreases to 2.08 V under illumination [42]. Still based on ZnS, a photocatalyst composed of CdSe/ZnS quantum dots with CNT (CdSe/ZnS QD@CNT) is developed, in which the QD and CNT networks provide pathways for transporting the electron-hole pairs, O_2, and Li^+. As shown in Fig. 3c, the QD nanoparticles are homogeneously distributed in the CNT network. The TEM image in Fig. 3d indicates that the CdSe/ZnS QD nanoparticles with the average particle size of 10±0.5 nm are well-attached to the CNT surfaces. When examining the photoelectrochemical performance of the composite, the charge voltage ends at 4.4 V without illumination, but reduces to 4.07 V under illumination. Moreover, the voltage profiles for 10 continuous charge-discharge cycling tests are stable. No matter with and without light, good stability is achieved for 100 cycles, demonstrating the potential for a real-time application.

Moreover, WO_3 nanowire arrays grown on carbon textile is also developed. As shown in Fig. 3e, the vertically grown WO_3 nanowires with the average length and diameter of several micrometers and 100 nm cover the surface of the carbon textiles. The HRTEM image in Fig. 3f shows the lattice spacing of 0.39 nm that corresponds to the (001) plane of the monoclinic WO_3. Owing to the visible light excited holes, the solid Li_2O_2 on the WO_3 nanowires can be effectively oxidized in the charge process. As shown in Fig. 5a, the charge and discharge voltages maintain at 3.55 V and 2.71 V even after 100 cycles, demonstrating high cycling stability (Fig. 5b). From Fig. 5c, the charge voltage is 3.41 V at 0.02 mA cm^{-1}, and still maintains below 3.84 V even at a

high current density of 0.10 mA cm^{-1}, while the discharge voltages maintain above 2.5 V at different current densities (Fig. 5d). Thus, good cycling stability and rate capability can be achieved using the WO_3 nanowire arrays.

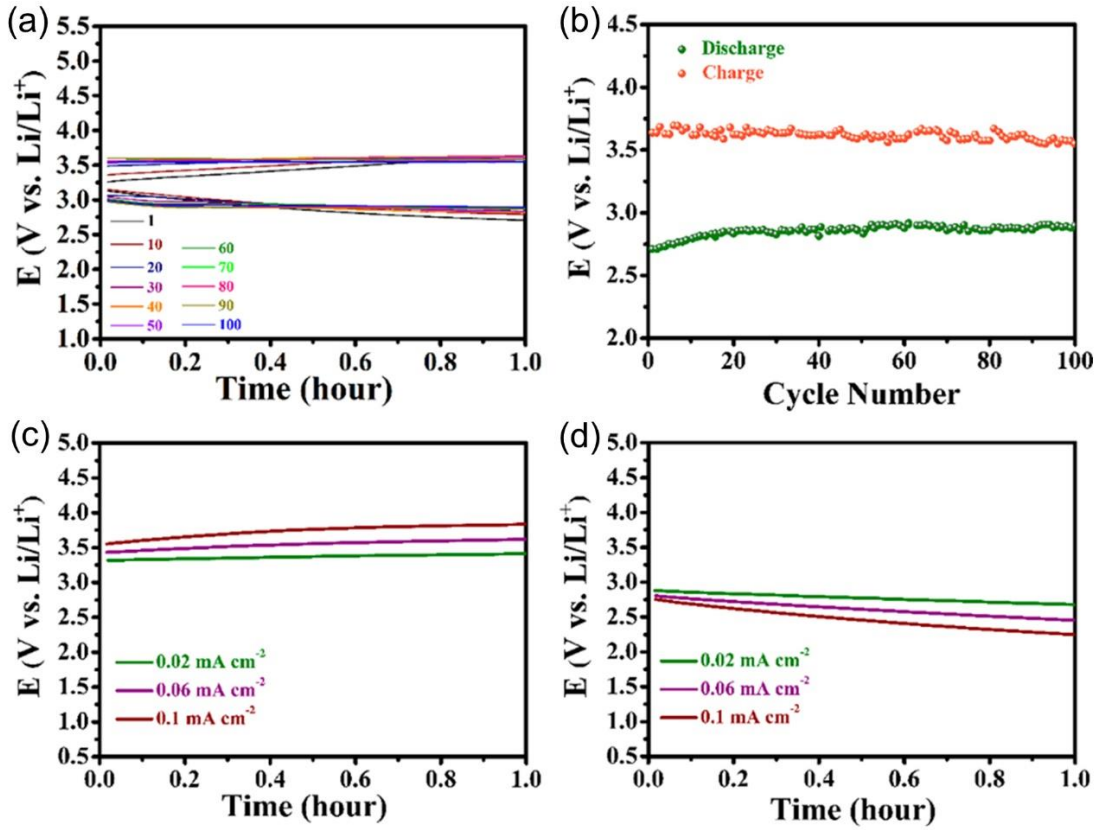

Fig. 5 Electrochemical performance of a Li-O_2 battery with the WO_3 nanowire arrays. (a) Voltage profiles for the charge and discharge processes and (b) Terminal voltages at 0.06 mA cm^{-2}. (c) Charge and (d) Discharge voltage profiles at different current densities. Reprinted with permission from Ref. [48].

From the above summary, most photocatalysts in Li-O_2 batteries are demonstrated to be effective in the charge process, while the functions in the discharge process remain unknown. In other types of metal-air batteries such as Zn-air batteries, a polymer semiconductor polytrithiophene can directly convert the photo-energy to electric energy during discharge [49], while the spinel-type cobalt

oxide can act as a photocatalyst for both discharge and charge [50]. Thus, a comprehensive investigation on the photocatalysts applied in Li-O_2 batteries is needed, which may further utilize the photo-energy and improve battery performance.

3.2 Electrolytes

Although the photocatalysts have significant roles in battery performance, the electrolyte can also affect the electrochemical behaviors [51–53]. As listed in Table 1, tetra-ethylene glycol dimethyl ether (TEGDME) has been widely used rather than dimethyl sulfoxide (DMSO) owing to its better stability [46]. Apart from the liquid electrolytes, a solid-state electrolyte membrane has also been made by dissolving lithium bis-trifluoromethanesulfonimide (LiTFSI) of 5 mol% into plastic crystal succinonitrile (SCN), through which a photo-assisted bendable Li-O_2 battery can achieve a charge voltage plateau of 2.15 V stably for 6 cycles [42]. However, the illumination can exacerbate the decomposition of electrolytes, resulting in poor cycle life [33]. The effects of different lithium salt concentrations on the photocatalytic degradation of electrolytes have been investigated [54]. Fig. 6a shows the Raman spectra of electrolytes with different mole ratios of LiTFSI: TEGDME. When the ratio is 1: 4, the diluted electrolyte is composed by solvent-separated-ion-pair. With the ratio gradually changes to 1:1, the blue shift of the S-N-S stretching mode and the increasing intensity of the Li^+-glyme-related peak (~875 cm^{-1}) indicates the formation of contacted-ion-pair (CIP) structure. Although the charge voltage profiles (Fig. 6b) and the X-ray diffraction (XRD) patterns (Fig. 6c) show only trace difference between the dilute (1:4) and the CIP-composed (1:1) electrolytes, the divergence in the

stability is observed by the spectroscopic results. As demonstrated in Fig. 6d, the residual Li_2O_2 and side-product Li_2CO_3 are evident after normal charging (N-Charge) in both electrolytes. While after photo-assisted charging (P-Charge), the peak intensities of side products (e.g., LiAc, $LiRCO_3$) are even higher in the dilute electrolyte (1:4), suggesting the effects of illumination on the electrolyte decomposition. For the CIP-composed electrolyte (1:1), the related peak intensities are greatly reduced, illustrating that the decomposition of the electrolyte can be restrained. Further, nuclear magnetic resonance (NMR) results in Fig. 6e shows the obvious reduction of carboxylates, confirming the enhanced stability of the CIP-composed electrolyte. Thus, developing stable electrolytes against photocatalytic degradation is crucial for battery stability, which requires more effort in future research.

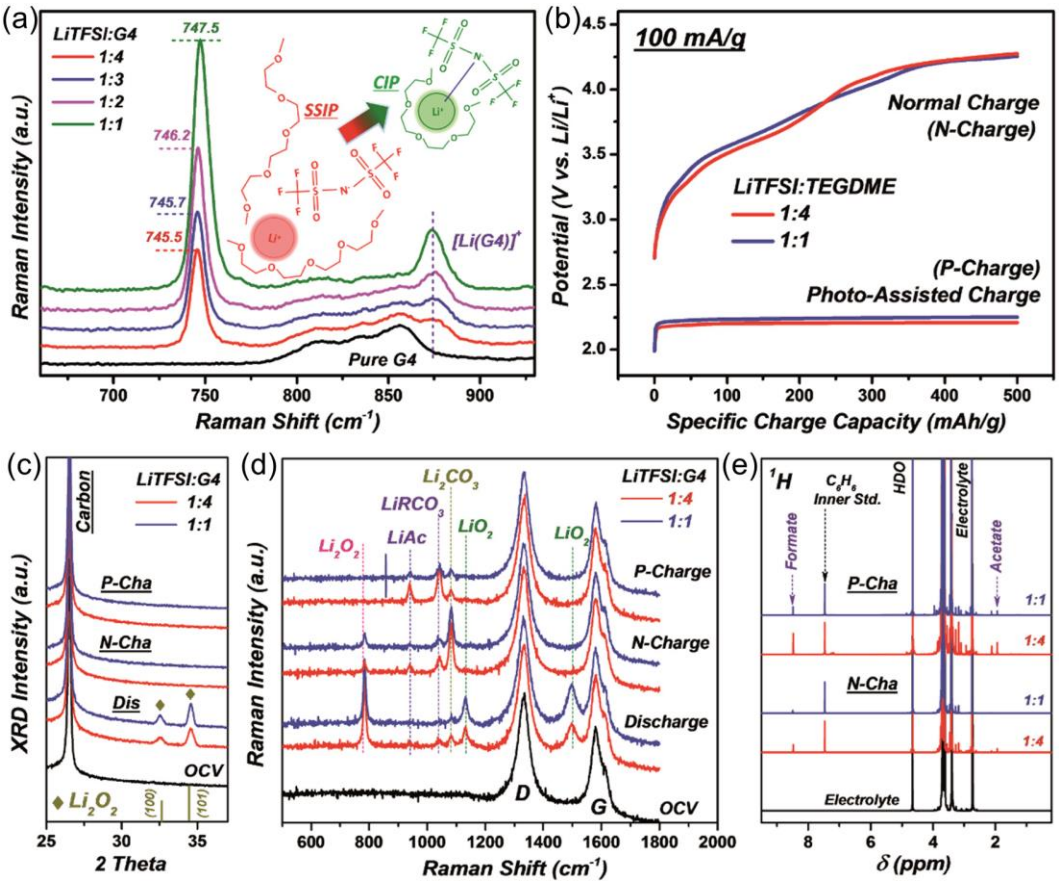

Fig. 6 Characterization and electrochemical performance of the electrolytes composed of different LiTFSI: TEGDME mole ratios. (a) Raman spectra. (b) Galvanostatic charge curves with and without photo assistant. (c) XRD patterns. (d) Ex-situ Raman spectra. (e) ^{1}H NMR of the electrodes collected from Li-O_2 batteries at corresponding discharge/charge states. Adapted with permission from Ref. [54].

4. Operating protocol

Although photo-assisted operating can effectively reduce the charge voltage, the illumination, especially for a long time, can cause the degradation of the electrode and electrolyte materials [33]. This may be one reason for the insufficient cycle life of most reported works. Besides improving the stability of battery materials, a novel method through changing the typical charging protocol to a hybrid strategy by

combining the typical and photo-assisted processes has been reported [54]. As schemed in Fig. 7a, for the conventional charge process, when the voltage is higher than 3.5 V, both the electrolyte and the electrode material (e.g., carbon) will be decomposed to form solid Li_2CO_3, decreasing the reversibility and greatly reducing the cycle life. When using the photo-assisted charging method, the degradation of electrolyte will occur under the long-time illumination, which is also harmful to the cycling stability. Thus, when introducing the photo-assisted charging process after the initial stage of conventional charging, as schemed in Fig. 7b, the formation of carbonate and carboxylates can be almost avoided owing to the low charge voltage and short illumination time, benefiting the cycle life. As demonstrated in Fig. 7c, the battery using the typical cycling charge protocol degrades at the 54^{th} cycle due to the accumulation of Li_2CO_3. While using a cut-off voltage of 3.5 V, the battery quickly degrades at the 24^{th} cycle due to the blockage of undecomposed Li_2O_2 on the active sites. When cycling with 5 conventional discharge-charge (1 h for discharge and 0.5 h for charge) cycles followed by a photo-assisted charging (2.5 h), the battery exhibits longer cycling life for over 150 cycles (300 h) with the charge voltage of lower than 3.5 V and a stable photo-assisted voltage of ~2.4 V.

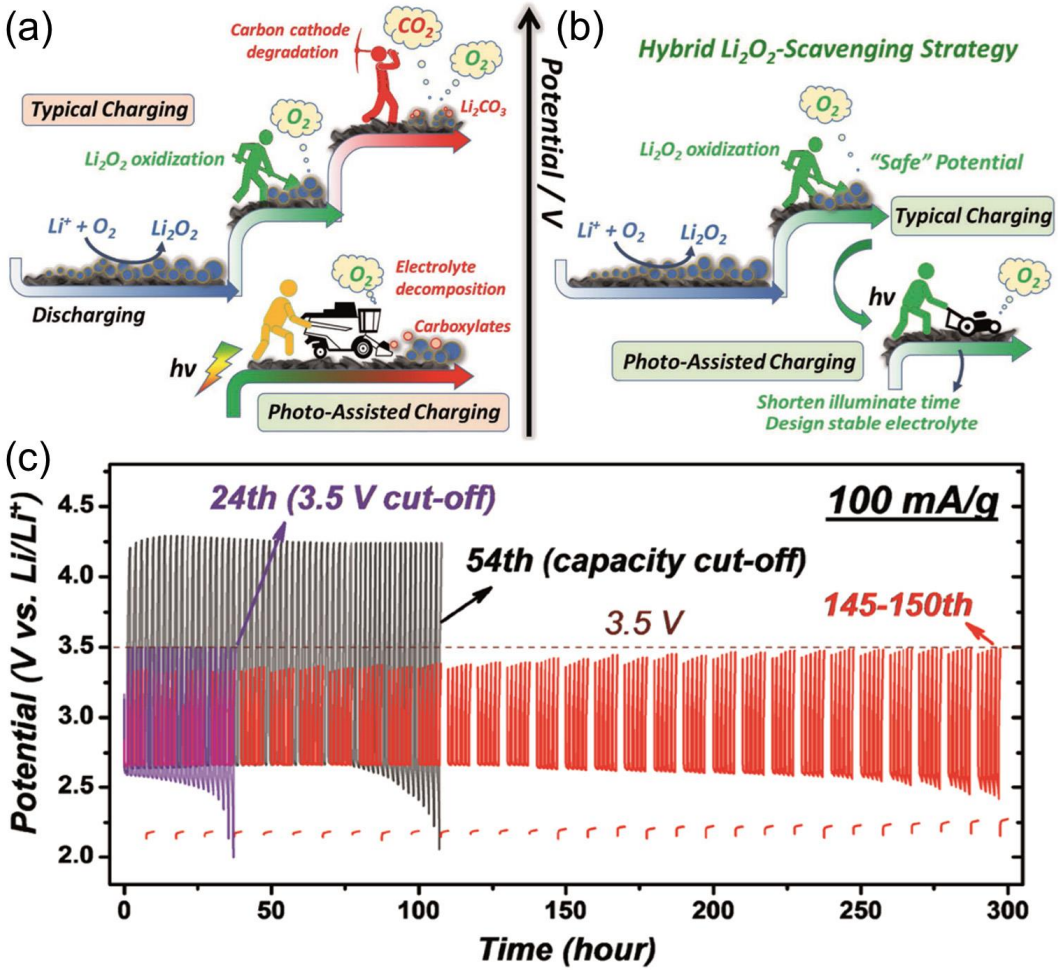

Fig. 7 Schematic illustration of (a) Conventional and photo-assisted charging processes and (b) hybrid charging. (c) Cycling behaviors of a Li-O_2 battery with photocatalysis operated with the hybrid charging strategy at 100 mAh g^{-1} (red curves). The cycling of the battery without photocatalysis is performed at a cut-off capacity of 100 mAh g^{-1} (black curves) and a cut-off voltage of 3.5 V (purple curves). Adapted with permission from Ref. [54].

Even the hybrid charging protocol has been proven to be an effective method to enhance the reversibility and cycle life, it should be noted that the overpotential still tends to increase during cycling, which is mainly caused by the accumulation of Li_2CO_3 [55–59]. Therefore, to fully refresh the oxygen electrode and enable a stable

cycling performance, a combination strategy may be applied, including applying stable electrolyte and electrode materials, hybrid charging protocol, and Li_2CO_3-scavenging catalysts (e.g., NiO) [60–62].

5. Conclusions and outlook

In conclusion, significant progress has been achieved in the photo-assisted non-aqueous Li-O_2 batteries in recent years, including the mechanism exploration, configuration design, material development, and operating protocol optimization. Through using photocatalyst to convert photo-energy into electricity, the electrochemical performance of the battery has been significantly improved, such as the low charge voltage (e.g., <2.0 V) and remarkable energy efficiency (e.g., >100%). While the existing problems are worth great attention for practical applications.

First, the stability of battery materials should be enhanced. As listed in Table 1, the reported cycle life is quite short when compared with conventional Li-O_2 batteries. Although the decomposition of electrolytes induced by illumination is one possible reason, the stability of photocatalysts in the discharge and charge conditions remains unknown, especially the synergetic effects of photocatalysts and electrolytes under the long-time illumination. In addition, metallic Li is directly used in which the light illumination is blocked by the separator. However, the parasitic reactions on the Li surface can occur due to the decomposition of electrolyte induced by the illumination, which may be one of the important subjects for the poor cycling stability. Hence, a comprehensive investigation on the stability of the Li electrode, electrolyte, and photocatalyst is essential.

Second, the electrode and battery structure should be greatly optimized. As a half-open system, the oxygen electrodes of photo-assisted Li-O_2 batteries should satisfy the exposition of both gas and light. To this end, the electrode should be built with highly porous and transparent materials to increase the oxygen transport pathway and illumination surface areas. Moreover, although the electric energy during charge is greatly reduced owing to the compensation of photo-energy, an external charging source is still needed. Thus, intelligent designs are needed to make the battery an energy self-sufficient system with the integration of photo-charging (e.g., solar to electric energy) and photo-assisted charging (e.g., solar to chemical energy) modules.

Third, the operating conditions should be carefully managed. As the photo-assisted charging should be conducted under illumination, the temperature of the battery may raise due to thermal irradiation (e.g., under solar light), which will change the electrochemical performance. However, the thermal effects have not been discussed yet, and the thermal properties of the battery materials remain unknown. Thus, effective thermal management is needed to enable stable operation. Additionally, owing to the intermittency of solar energy, the photo-assisted charging process may be interrupted irregularly when using solar light, causing the fluctuation of the charge voltage. To this end, effective voltage compensation is needed to stabilize the operation.

In summary, the research of photo-assisted non-aqueous Li-O_2 batteries is still in the early stage. With research efforts, it is believed that combining photochemistry and Li-O_2 batteries will provide a novel and effective strategy for energy storage and

conversion, especially for solar energy utilization. The insight obtained from these investigations will also benefit other novel energy conversion and storage systems.

Abbreviations

CB	Conduction band
CIP	Contacted-ion-pair
CNT	Carbon nanotube
DMSO	Dimethyl sulfoxide
HRTEM	High-resolution transmission electron microscope
LiTFSI	Lithium bis-trifluoromethanesulfonimide
M^{ox}	Oxidized form of redox mediator
M^{red}	Reduced form of redox mediator
NMR	Nuclear magnetic resonance
QD	Quantum dot
SCN	Succinonitrile
SEM	Scan electron microscope
TEGDME	Tetra-ethylene glycol dimethyl ether
TEM	Transmission electron microscope
VB	Valence band
VRFB	Vanadium redox flow battery
XRD	X-ray diffraction

Author contributions

Peng Tan: Conceptualization; Funding acquisition; Supervision; Writing -

original draft, review & editing. **Xu Xiao:** Writing - review & editing. **Yawen Dai:** Writing - review & editing. **Chun Cheng:** Writing - review & editing. **Meng Ni:** Funding acquisition; Supervision; Writing - review & editing.

Declaration of interest

None.

Acknowledgments

Peng Tan thanks the funding support from CAS Pioneer Hundred Talents Program (KJ2090130001) and USTC Tang Scholar. Meng Ni thanks the funding support from The Hong Kong Polytechnic University (G-YW2D), and a grant (Project Number: PolyU 152214/17E) from Research Grant Council, University Grants Committee, Hong Kong SAR.

References

[1] Kabir E, Kumar P, Kumar S, Adelodun AA, Kim K-H. Solar energy: Potential and future prospects. Renew Sustain Energy Rev 2018;82:894–900.

[2] Sampaio PGV, González MOA. Photovoltaic solar energy: Conceptual framework. Renew Sustain Energy Rev 2017;74:590–601.

[3] Zhang T, Yan Z, Pei G, Zhu Q, Ji J. Experimental optimization on the volume-filling ratio of a loop thermosyphon photovoltaic/thermal system. Renew Energy 2019;143:233–42.

[4] Wang Q, Hu M, Yang H, Cao J, Li J, Su Y, et al. Energetic and exergetic analyses on structural optimized parabolic trough solar receivers in a concentrated solar–thermal collector system. Energy 2019;171:611–23.

[5] Sánchez-Pantoja N, Vidal R, Pastor MC. Aesthetic impact of solar energy systems. Renew Sustain Energy Rev 2018;98:227–38.

[6] Yu M, McCulloch WD, Huang Z, Trang BB, Lu J, Amine K, et al. Solar-powered electrochemical energy storage: An alternative to solar fuels. J Mater Chem A 2016;4:2766–82.

[7] Dunn B, Kamath H, Tarascon J-M. Electrical Energy Storage for the Grid: A Battery of Choices. Science 2011;334:928–35.

[8] Zhao P, Zhang H, Zhou H, Chen J, Gao S, Yi B. Characteristics and performance of 10 kW class all-vanadium redox-flow battery stack. J Power Sources 2006;162:1416–20.

[9] Wu Q, Zhang X, Lv Y, Lin L, Liu Y, Zhou X. Bio-inspired multiscale-pore-network structured carbon felt with enhanced mass transfer and activity for vanadium redox flow batteries. J Mater Chem A 2018;6:20347–55.

[10] Zeng Y, Li F, Lu F, Zhou X, Yuan Y, Cao X, et al. A hierarchical interdigitated flow field design for scale-up of high-performance redox flow batteries. Appl Energy 2019;238:435–41.

[11] Wu Q, Lv Y, Lin L, Zhang X, Liu Y, Zhou X. An improved thin-film electrode for vanadium redox flow batteries enabled by a dual layered structure. J Power Sources 2019;410–411:152–61.

[12] Skyllas-Kazacos M, Chakrabarti MH, Hajimolana SA, Mjalli FS, Saleem M. Progress in Flow Battery Research and Development. J Electrochem Soc 2011;158:R55–79.

[13] Balogun M-S, Qiu W, Wang W, Fang P, Lu X, Tong Y. Recent advances in metal nitrides as high-performance electrode materials for energy storage devices. J Mater Chem A 2015;3:1364–87.

[14] Cheng F, Chen J. Metal–air batteries: from oxygen reduction electrochemistry to cathode catalysts. Chem Soc Rev 2012;41:2172–92.

[15] Li Y, Lu J. Metal–Air Batteries: Will They Be the Future Electrochemical Energy Storage Device of Choice? ACS Energy Lett 2017;2:1370–7.

[16] Rahman MA, Wang X, Wen C. High Energy Density Metal-Air Batteries: A Review. J Electrochem Soc 2013;160:A1759–71.

[17] Tan P, Jiang HR, Zhu XB, An L, Jung CY, Wu MC, et al. Advances and challenges in lithium-air batteries. Appl Energy 2017;204:780–806.

[18] Bruce PG, Freunberger SA, Hardwick LJ, Tarascon J-M. Li-O_2 and Li-S batteries with high energy storage. Nat Mater 2012;11:19–29.

[19] Gurung A, Qiao Q. Solar Charging Batteries: Advances, Challenges, and Opportunities. Joule 2018;2:1217–30.

[20] Pena-Bello A, Barbour E, Gonzalez MC, Patel MK, Parra D. Optimized PV-coupled battery systems for combining applications: Impact of battery technology and geography. Renew Sustain Energy Rev 2019;112:978–90.

[21] Gibson TL, Kelly NA. Solar photovoltaic charging of lithium-ion batteries. J Power Sources 2010;195:3928–32.

[22] Xu J, Chen Y, Dai L. Efficiently photo-charging lithium-ion battery by perovskite solar cell. Nat Commun 2015;6:8103.

[23] Li Q, Li N, Liu Y, Wang Y, Zhou H. High-Safety and Low-Cost Photoassisted Chargeable Aqueous Sodium-Ion Batteries with 90% Input Electric Energy Savings. Adv Energy Mater 2016;6:1600632.

[24] Paolella A, Faure C, Bertoni G, Marras S, Guerfi A, Darwiche A, et al. Light-assisted delithiation of lithium iron phosphate nanocrystals towards photo-rechargeable lithium ion batteries. Nat Commun 2017;8:14643.

[25] Li Q, Liu Y, Guo S, Zhou H. Solar energy storage in the rechargeable batteries. Nano Today 2017;16:46–60.

[26] Jung K-N, Kim J, Yamauchi Y, Park M-S, Lee J-W, Kim JH. Rechargeable lithium–air batteries: a perspective on the development of oxygen electrodes. J Mater Chem A 2016;4:14050–68.

[27] Liu B, Yan P, Xu W, Zheng J, He Y, Luo L, et al. Electrochemically Formed Ultrafine Metal Oxide Nanocatalysts for High-Performance Lithium-Oxygen Batteries. Nano Lett 2016;16:4932–9.

[28] Jung J-W, Im H-G, Lee D, Yu S, Jang J-H, Yoon KR, et al. Conducting Nanopaper: A Carbon-Free Cathode Platform for Li–O_2 Batteries. ACS Energy Lett 2017;2:673–80.

[29] Tan P, Liu M, Shao Z, Ni M. Recent Advances in Perovskite Oxides as Electrode Materials for Nonaqueous Lithium–Oxygen Batteries. Adv Energy Mater 2017;7:1–23.

[30] Bergner BJ, Schürmann A, Peppler K, Garsuch A, Janek J. TEMPO: A Mobile Catalyst for Rechargeable Li-O_2 Batteries. J Am Chem Soc

2014;136:15054–64.

[31] Chen Y, Freunberger S a, Peng Z, Fontaine O, Bruce PG. Charging a Li-O_2 battery using a redox mediator. Nat Chem 2013;5:489–94.

[32] Hirshberg D, Kwak W-J, Sharon D, Afri M, Frimer AA, Jung H-G, et al. Li-O_2 cells with LiBr as an Electrolyte and Redox Mediator. Energy Environ Sci 2016;9:2334–45.

[33] Yu M, Ren X, Ma L, Wu Y. Integrating a redox-coupled dye-sensitized photoelectrode into a lithium-oxygen battery for photoassisted charging. Nat Commun 2014;5:1–6.

[34] Liu Y, Li N, Liao K, Li Q, Ishida M, Zhou H. Lowering the charge voltage of Li-O2 batteries: Via an unmediated photoelectrochemical oxidation approach. J Mater Chem A 2016;4:12411–5.

[35] Lee CK, Park YJ. CsI as Multifunctional Redox Mediator for Enhanced Li-Air Batteries. ACS Appl Mater Interfaces 2016;8:8561–7.

[36] Zhang T, Liao K, He P, Zhou H. A self-defense redox mediator for efficient lithium-O_2 batteries. Energy Environ Sci 2016;9:1024–30.

[37] Landa-Medrano I, Olivares-Marín M, Pinedo R, Ruiz De Larramendi I, Rojo T, Tonti D. Operando UV-visible spectroscopy evidence of the reactions of iodide as redox mediator in Li-O_2 batteries. Electrochem Commun 2015;59:24–7.

[38] Bergner BJ, Hofmann C, Schürmann A, Schröder D, Peppler K, Schreiner PR, et al. Understanding the Fundamentals of Redox Mediators in Li-O_2 Batteries: A Case Study on Nitroxides. Phys Chem Chem Phys 2015;17:31769–79.

[39] Liu Y, Li N, Wu S, Liao K, Zhu K, Yi J, et al. Reducing the charging voltage of a Li–O_2 battery to 1.9 V by incorporating a photocatalyst. Energy Environ Sci 2015;8:2664–7.

[40] Xu W, Wang J, Ding F, Chen X, Nasybulin E, Zhang Y, et al. Lithium metal anodes for rechargeable batteries. Energy Environ Sci 2014;7:513–37.

[41] Aurbach D, Zinigrad E, Cohen Y, Teller H. A short review of failure mechanisms of lithium metal and lithiated graphite anodes in liquid electrolyte solutions. Solid State Ionics 2002;148:405–16.

[42] Liu Y, Yi J, Qiao Y, Wang D, He P, Li Q, et al. Solar-driven efficient Li_2O_2 oxidation in solid-state Li-ion O_2 batteries. Energy Storage Mater 2018;11:170–5.

[43] Gong H, Wang T, Xue H, Fan X, Gao B, Zhang H, et al. Photo-enhanced lithium oxygen batteries with defective titanium oxide as both photo-anode and air electrode. Energy Storage Mater 2018;13:49–56.

[44] Yang X yang, Feng X lan, Jin X, Shao M zhe, Yan B lin, Yan J min, et al. An Illumination-Assisted Flexible Self-Powered Energy System Based on a Li–O_2 Battery. Angew Chemie Int Ed 2019;58:16411–5.

[45] Zhu Z, Shi X, Fan G, Li F, Chen J. Photo-energy Conversion and Storage in an Aprotic Li-O_2 Battery. Angew Chemie Int Ed 2019;58:19021–6.

[46] Kumar S, Jena A, Hu YC, Liang C, Zhou W, Hung TF, et al. Cobalt Diselenide Nanorods Grafted on Graphitic Carbon Nitride: A Synergistic Catalyst for Oxygen Reactions in Rechargeable Li−O_2 Batteries. ChemElectroChem

2018;5:5.

[47] Veeramani V, Chen YH, Wang HC, Hung TF, Chang WS, Wei DH, et al. CdSe/ZnS QD@CNT nanocomposite photocathode for improvement on charge overpotential in photoelectrochemical Li-O_2 batteries. Chem Eng J 2018;349:235–40.

[48] Feng Y, Xue H, Wang T, Gong H, Gao B, Xia W, et al. Enhanced Li_2O_2 Decomposition in Rechargeable Li-O_2 Battery by Incorporating WO_3 Nanowire Array Photocatalyst. ACS Sustain Chem Eng 2019;7:5931–9.

[49] Zhu D, Zhao Q, Fan G, Shuo Z, Wang L, Li F, et al. Photo-Induced Oxygen Reduction Reaction Boosts The Output Voltage of Zn-Air Battery. Angew Chemie Int Ed 2019;58:12460.

[50] Tomon C, Sarawutanukul S, Duangdangchote S, Krittayavathananon A, Sawangphruk M. Photoactive Zn-air batteries using spinel-type cobalt oxide as a bifunctional photocatalyst at the air cathode. Chem Commun 2019;55:5855–8.

[51] Luntz AC, McCloskey BD. Nonaqueous Li-air batteries: A status report. Chem Rev 2014;114:11721–50.

[52] Balaish M, Kraytsberg A, Ein-Eli Y. A critical review on lithium-air battery electrolytes. Phys Chem Chem Phys 2014;16:2801–22.

[53] Lai J, Xing Y, Chen N, Li L, Wu F, Chen R. A comprehensive insight into the electrolytes for rechargeable lithium-air batteries. Angew Chemie Int Ed 2020;59:2974.

[54] Qiao Y, Liu Y, Jiang K, Li X, He Y, Li Q, et al. Boosting the Cycle Life of

Aprotic Li-O_2 Batteries via a Photo-Assisted Hybrid Li_2O_2-Scavenging Strategy. Small Methods 2018;2:1700284.

[55] Tan P, Shyy W, Wei ZH, An L, Zhao TS. A carbon powder-nanotube composite cathode for non-aqueous lithium-air batteries. Electrochim Acta 2014;147:1–8.

[56] Cao Y, Zheng M, Cai S, Lin X, Yang C, Hu W, et al. Carbon embedded α-MnO_2@graphene nanosheet composite: a bifunctional catalyst for high performance lithium oxygen batteries. J Mater Chem A 2014;2:18736–41.

[57] Balasubramanian P, Marinaro M, Theil S, Wohlfahrt-Mehrens M, Jörissen L. Au-coated carbon electrodes for aprotic Li-O_2 batteries with extended cycle life: The key issue of the Li-ion source. J Power Sources 2015;278:156–62.

[58] McCloskey BD, Speidel A, Scheffler R, Miller DC, Viswanathan V, Hummelshøj JS, et al. Twin problems of interfacial carbonate formation in nonaqueous Li-O_2 batteries. J Phys Chem Lett 2012;3:997–1001.

[59] Meini S, Tsiouvaras N, Schwenke KU, Piana M, Beyer H, Lange L, et al. Rechargeability of Li-air cathodes pre-filled with discharge products using an ether-based electrolyte solution: implications for cycle-life of Li-air cells. Phys Chem Chem Phys 2013;15:11478–93.

[60] Tan P, Wei ZH, Shyy W, Zhao TS, Zhu XB. A nano-structured RuO_2/NiO cathode enables the operation of non-aqueous lithium-air batteries in ambient air. Energy Environ Sci 2016;9:1783–93.

[61] Wang R, Yu X, Bai J, Li H, Huang X, Chen L, et al. Electrochemical decomposition of Li_2CO_3 in NiO-Li_2CO_3 nanocomposite thin film and powder

electrodes. J Power Sources 2012;218:113–8.

[62] Song S, Xu W, Zheng J, Luo L, Engelhard MH, Bowden ME, et al. Complete Decomposition of Li_2CO_3 in Li–O_2 Batteries Using Ir/B_4C as Noncarbon-Based Oxygen Electrode. Nano Lett 2017;17:1417–24.